Chapter 5

Methane on Microporous Carbons

N.P. Stadie, M. Murialdo, C.C. Ahn, and B. Fultz, "Unusual Entropy of Adsorbed Methane on Zeolite-Templated Carbon," J. Phys. Chem. C, 119, 26409 (2015).
DOI: 10.1021/acs.jpcc.5b05021
http://pubs.acs.org/doi/abs/10.1021/acs.jpcc.5b05021?journalCode=jpccck

N.P. Stadie, M. Murialdo, C.C. Ahn, and B. Fultz, "Anomalous Isosteric Enthalpy of Adsorption of Methane on Zeolite-Templated Carbon," J. Am. Chem. Soc. 135, 990 (2013).
DOI: 10.1021/ja311415m
http://pubs.acs.org/doi/abs/10.1021/ja311415m

1. Adsorptive Uptake

The ability to store the necessary quantities of natural gas in inexpensive and moderately sized onboard tanks remains a significant challenge to the wide-spread adoption of natural gas as a fuel in the transportation sector. By filling the onboard tanks with specially designed physisorptive materials, the storage capacity can be significantly improved and the volumetric energy density significantly increased. Here we study high-pressure methane adsorption on three microporous carbons (ZTC, MSC-30, and CNS-201). The zeolite-templated carbon (ZTC) is of particular interest due to its unique synthesis and morphology (a narrow pore-size distribution centered at 1.2 nm).

Methane isotherms were measured at 13 temperatures from 238 to 526K and up to pressures of ~10 MPa in a volumetric Sieverts apparatus, commission and verified for accurate measurements up to 10 MPa[1]. Multiple adsorption runs were completed at each temperature

with research-grade methane (99.999%) and errors between cycles were less than 1%. Adsorption/desorption cycles demonstrated full reversibility of the isotherms. The excess adsorption isotherms are plotted in Figure 1. Unlike absolute adsorption, excess adsorption reaches a maximum at high pressures. This maximum is a readily accessible figure of merit for the gravimetric performance of a material at a fixed temperature. The excess maximum is similar for ZTC-3 and MSC-30 at room temperature, but slightly higher for MSC-30 at 14.5 mmol g^{-1} at 8 MPa. While excess adsorption increases faster for MSC-30 at pressures between 0 and 0.8 MPa, uptake in ZTC-3 increases fastest between 0.8 and 5.7 MPa. CNS-201 has much lower maxima due to its significantly smaller surface area. The highest measured excess uptake of this study is for ZTC-3 at 238 K: 22.1 mmol g^{-1} (26.2 wt%) at 4.7 MPa, despite a gentler initial increase at low pressure. Interestingly, the excess uptake in ZTC-3 is also greater than for MSC-30 at high temperatures, although neither reaches a maximum between 0 and 9 MPa. At all temperatures, methane uptake in ZTC-3 is characterized by a gradual initial rise and delayed increase at pressures between 0.2 and 2 MPa, leading to higher eventual methane capacity than MSC-30, a material of comparable specific surface area. The measured excess adsorption maxima (at a sample temperature of 298K) scale linearly with specific surface area and are consistent with the reported linear trend for methane uptake at 3.5 MPa and 298 K.[2]

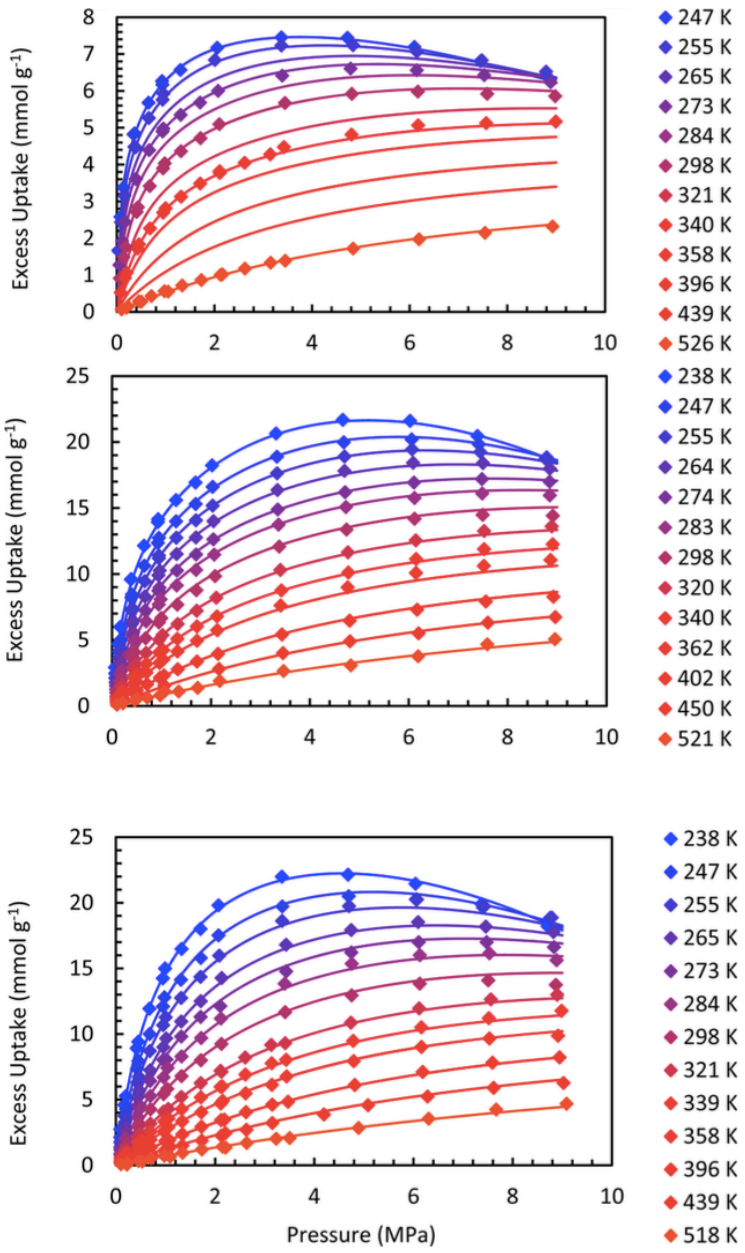

Figure 1. Measured methane excess adsorption as a function of temperature and pressure on CNS-201 (top), MSC-30 (middle), and ZTC (bottom). The curves indicate the best fit obtained with a dual-Langmuir fitting function.

2. Analysis

The excess adsorption data were fitted with a superposition of two Langmuir isotherms, as detailed in Chapter 3. In general, the best-fit parameters obtained correlate with physical properties of the materials studied. For example, the parameter indicative of the maximum volume of the adsorbed layer, V_{max}, can be independently verified through comparison to the micropore volume of the adsorbent as measured with the Dubinin-Radushkevich method[3,4]. In ZTC, if taken to be proportional to surface area, the V_{max} parameter corresponds to half of the mean pore width of the material: a thickness of 0.6 nm. Likewise, the maximum possible adsorption quantity, given by parameter n_{max}, correlates well with an estimate determined by the product of the micropore volume and the molar liquid density of the adsorbate (methane)[5].

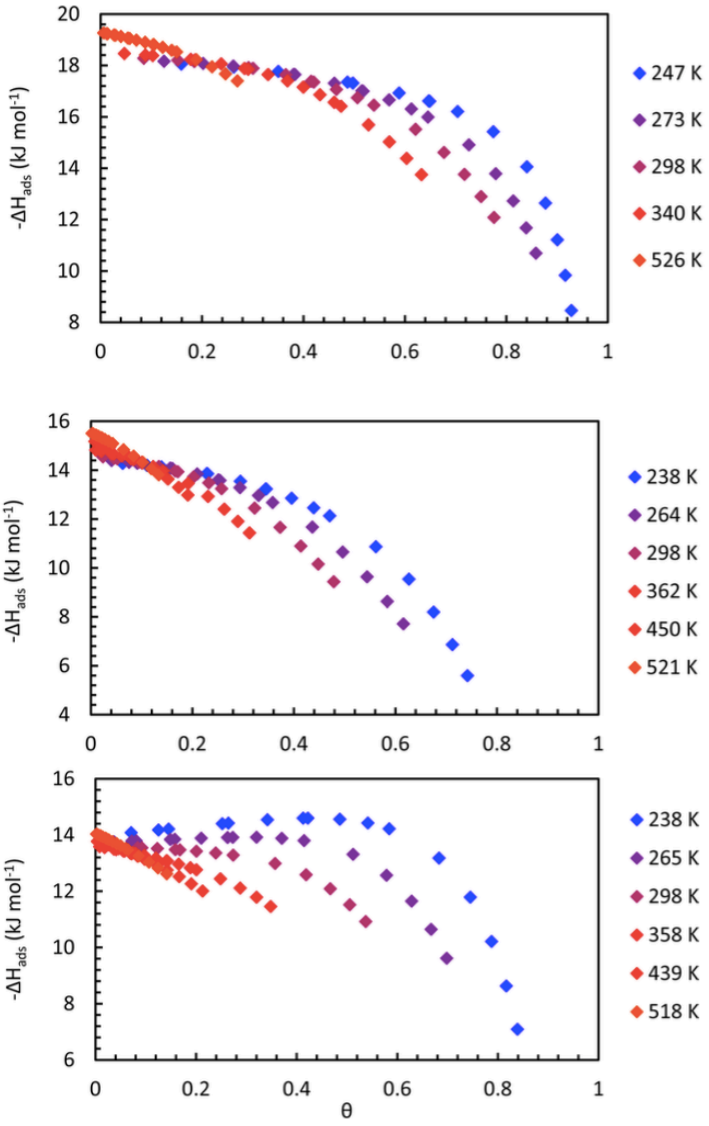

Figure 2. The isosteric heats of methane adsorption on CNS-201 (top), MSC-30 (middle), and ZTC (bottom) as a function of temperature and fractional site occupancy (θ).

The isosteric enthalpy of adsorption is the molar change in enthalpy of the adsorptive species upon adsorption. While adsorption is an exothermic process, the isosteric heat of adsorption is reported as a positive quantity by convention, as shown in Figure 2. These curves were obtained by applying the Clapeyron relationship to the dual-Langmuir fits. It is necessary to use the general form of the Clapeyron relationship for methane adsorption at high pressure

because of the significant nonideality of methane gas-state properties. Its derivation and explanation with respect to the ideal-gas form of the equation are given in Chapter 3.

The Henry's Law value of adsorption heat, $-\Delta H_0$, is calculated by extrapolating the heat of adsorption to zero pressure. The Henry's law values for CNS-201, MSC-30, and ZTC-3 are 18.1-19.3, 14.4-15.5, and 13.5-14.2 kJ mol^{-1}, respectively. The isosteric heats of methane adsorption as a function of fractional occupancy, θ, in the activated carbons (CNS-201 and MSC-30) are typical of other carbon materials, with the isosteric heats decreasing with θ. In the range $0 < \theta < 0.6$, the more graphitic CNS-201 shows a more gradual decrease of isosteric heat than MSC-30, indicative of more heterogeneous site energies in MSC-30. Surprisingly, the isosteric heat of adsorption in ZTC increases to a maximum at θ = 0.5-0.6 at temperatures from 238 to 273 K. This increase is anomalous compared to previous experimental reports of methane adsorption on carbon.

This anomalous effect results from adsorbate-adsorbate intermolecular interactions, as suggested by theoretical work.[6,7,8] We have reported similar effects for ethane (Chapter 6) and krypton (Chapter 7). Accurately assessing the contribution of intermolecular interactions to the isosteric heat requires knowledge of the adsorption binding-site energies. A heterogeneous distribution of site energies, as in MSC-30, is reflected in the relatively rapid decrease of the isosteric heat with θ. This behavior is common as the most favorable sites are filled first (on average). The material properties of ZTC, including a narrow distribution of pore width, periodic pore spacing, and high content of sp^2-hybridized carbon, suggest a high degree of homogeneity of the binding-site energies. We expect that the measured increase of 0.5 kJ mol^{-1} in the isosteric heat at 238K reflects most of the contribution from favorable intermolecular

interactions, and this increase is in good agreement with calculations of lateral interactions of methane molecules on a surface.[6,7] An increasing isosteric heat, as seen with methane on ZTC, is highly desirable as it enhances deliverable storage capacity. This effect enables a larger fraction of the adsorption capacity at pressures above the lower bound of useful storage. Indeed, the deliverable gravimetric methane capacities of ZTC at temperatures near ambient are the highest of any reported carbonaceous material.

A clearer picture of adsorption thermodynamics can be achieved by evaluating the specific enthalpy of the adsorbed phase, as shown in Figure 3. This removes the gas-phase dependency of the isosteric heat and focuses solely on adsorbed-phase thermodynamics. This is particularly useful because at a constant temperature, it is a reasonable approximation that the specific properties of the adsorbed phase as a function of increasing site occupancy do not depend on contributions from internal (intramolecular) phenomena. Here, a decreasing enthalpy of the adsorbed phase as a function of uptake, as seen on ZTC, corresponds to an "increasing" (or, decreasing negative) isosteric heat of adsorption.

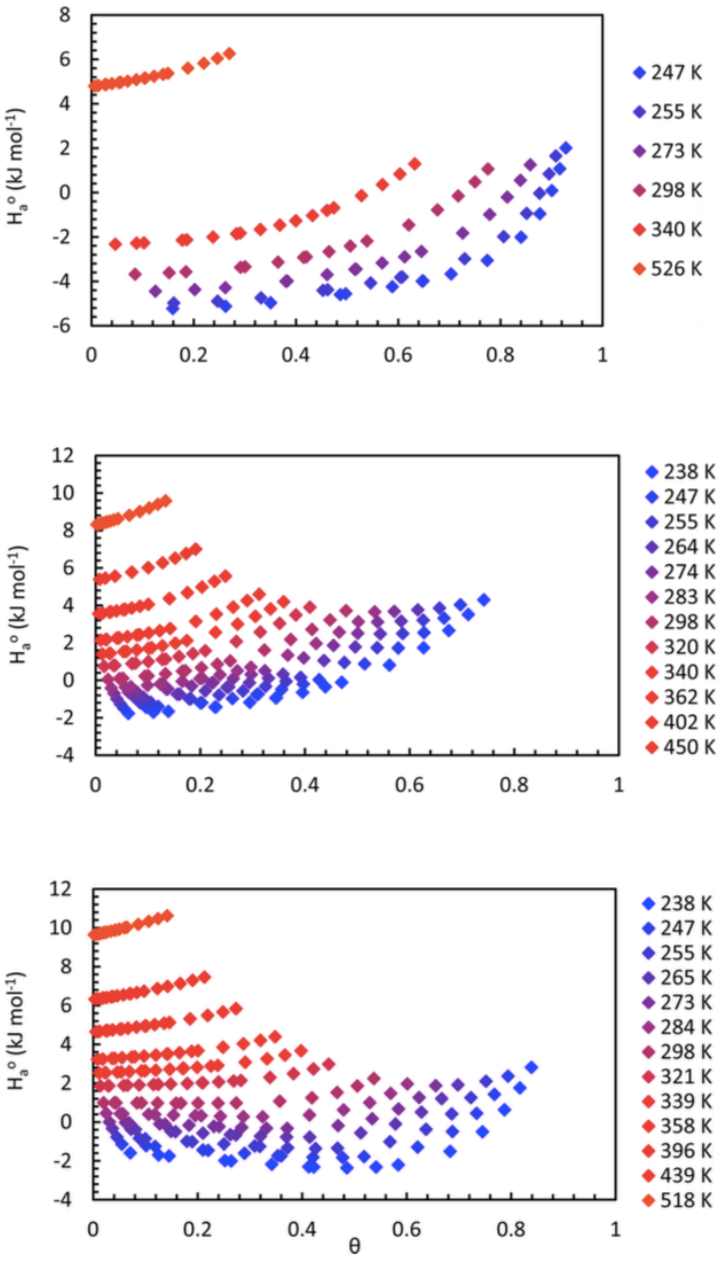

Figure 3. Adsorbed-phase enthalpy of CNS-201 (top), MSC-30 (middle), and ZTC (bottom) as a function of temperature and fractional occupancy (θ).

The adsorbed-phase entropy was determined in a similar manner that is described in more detail in Chapter 3. Adsorbed-phase entropy isotherms are shown in Figure 4. While all

three adsorbed phases show qualitatively similar entropies, a notable difference is seen between the smaller pore materials (CNS-201 and ZTC) and MSC-30, which has a significant fraction of pores of widths >2 nm. The molar entropy of methane adsorbed on CNS- 201 and ZTC at 238 K approaches the value of the liquid reference state rather closely (within 12 J K^{-1} mol^{-1}), indicating a liquid-like character of the adsorbed layer, unlike on MSC-30 (reaching a minimum of 22 J K^{-1} mol^{-1} at 238 K). We must note, however, the relatively arbitrary nature of the reference state; the entropy of saturated liquid CH_4 varies by ~45 J K^{-1} mol^{-1} along its liquidus phase boundary.

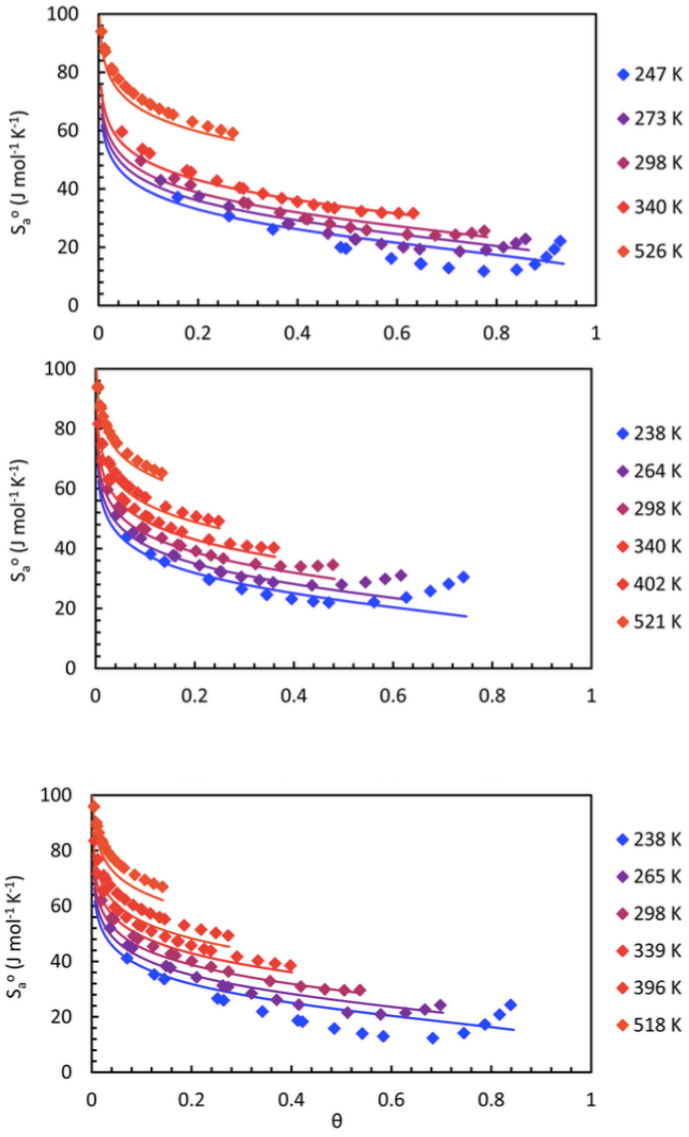

Figure 4. Adsorbed-Phase Entropy of methane on CNS-201 (top), MSC-30 (middle), and ZTC (bottom) as a function of temperature and fractional occupancy. Curves indicate corresponding statistical mechanics estimates.

For comparison, statistical mechanics calculations were carried out to independently estimate the adsorbed-phase entropy. The only experimental parameter used in the theoretical calculations was the material's specific surface area. A remarkable consistency between theory

and experiment is observed across all three adsorbents, especially in the limit of high temperature and low pressure where the approximations in the theoretical model are most justified[9]. Of particular note, the theoretical calculations very closely reproduce the measured molar entropies of the adsorbed phase on MSC-30, where the largest errors between θ = 0-0.2 are <3.5% at all temperatures measured (see Figure 4). The agreement between experimental data and the statistical mechanical calculations for the adsorbed phase on CNS-201 is similarly close in the dilute limit, but strays significantly beyond θ = 0.35. On ZTC, however, the estimated adsorbed-phase entropy exceeds measured values, especially at low temperatures and moderate coverage. This suggests the mechanism by which enhanced adsorbate-adsorbate interactions are promoted in the adsorbed phase on ZTC, namely clustered configurations.

For ZTC, confinement of an adsorbed phase in narrow pores is likely to lead to clustering as a result of enhanced lateral interactions. The formation of such clusters, or adsorbate "islands", on an adsorbent surface due to attractive intermolecular interactions, is a well-known feature of physisorption of strongly interacting molecular species (e.g., methanol on indium-tin-oxide glass[10]) and moderately interacting molecular species (e.g., subcritical CO_2 on several MOFs and zeolites[11,12]) and also of chemisorption of fairly weakly interacting atomic species (e.g., oxygen on Pt(111)[13]). This clustering behavior results in a reduction in entropy due to the reduced number of accessible configurations of the cluster(s) in the same total number of sites. This is consistent with the reduced entropy measured for methane on ZTC as compared to the statistical mechanics estimate. The topic of clustering accounting for enhanced adsorbate-adsorbate interactions is investigated in more detail in Chapter 8.

As a general note, the entropies of methane adsorbed between 238 and 526 K on the

various carbon materials measured in this work are very high as compared to some historical theoretical estimates, approaching values of bulk gaseous methane in the dilute limit. In fact, this observation has recently been made across many materials and adsorbed molecular species.[14] The ratio of adsorbed-phase entropy to the gas-phase entropy for CH_4 on MSC-30, for example, spans from 0.3 (at 238 K and 2 MPa) to 0.8 (at 0.1 MPa and 521 K), similar to the value reported for methane on graphite(0001) in the dilute limit: 0.76 at 55 K.[14,15]

References:

1. Bowman, R. C.; Luo, C. H.; Ahn, C. C.; Witham, C. K.; Fultz, B. The Effect of Tin on the Degradation of LaNi5-ySny Metal-Hydrides During Thermal Cycling. *J. Alloys Compd.* **1995**, *217*, 185-192.
2. Sun, Y.; Liu, C. M.; Su, W.; Zhou, Y. P.; Zhou, L. Principles of Methane Adsorption and Natural Gas Storage. *Adsorption.* **2009**, *15*, 133-137.
3. Dubinin, M. M.; Radushkevich, L. V. Equation of the Characteristic Curve of Activated Charcoal. *Proc. Acad. Sci. USSR Phys. Chem. Sect.* **1947**, 55, 331-337.
4. Burevski, D. The Application of the Dubinin-Astakhov Equation to the Characterization of Microporous Carbons. *Colloid Polym. Sci.* **1982,** *260*, 623-627.
5. Lemmon, E. W.; Huber, M. L.; McLinden, M. O. *NIST Standard Reference Database 23: Reference Fluid Thermodynamic and Transport Properties-REFPROP*, Version 8.0 [CD-ROM], 2007.
6. Salem, M. M. K.; Braeuer, P.; von Szombathely, M.; Heuchel, M.; Harting, P.; Quitzsch, K.; Jaroniec, M. Thermodynamics of High-Pressure Adsorption of Argon, Nitrogen, and Methane on Microporous Adsorbents. *Langmuir.* **1998**, *14*, 3376-3389.
7. Sillar, K.; Sauer, J. Ab Initio Prediction of Adsorption Isotherms for Small Molecules in Metal-Organic Frameworks: The Effect of Lateral Interactions for Methane/CPO-27-Mg. *J. Am. Chem. Soc.* **2012**, *134*, 18354-18365.
8. Al-Muhtaseb, S. A.; Ritter, J. A. Roles of Surface Heterogeneity and Lateral Interactions on the Isosteric Heat of Adsorption and Adsorbed Phase Heat Capacity. *J. Phys. Chem. B.* **1999**, *103*, 2467-2479.
9. Stadie, N. P.; Murialdo, M.; Ahn, C. C.; Fultz, B. Unusual Entropy of Adsorbed Methane on Zeolite-Templated Carbon. *J. Phys. Chem. C* **2015**, *119,* 26409-26421.
10. Wang, L.; Song, Y. H.; Wu, A. G.; Li, Z.; Zhang, B. L.; Wang, E. K. Study of Methanol Adsorption on Mica, Graphite and ITO Glass by Using Tapping Mode Atomic Force Microscopy. *Appl. Surf. Sci.* **2002**, *199*, 67-73.
11. Krishna, R.; van Baten, J. A. Investigating Cluster Formation in Adsorption of CO2, CH4, and Ar in Zeolites and Metal Organic Frameworks at Suberitical Temperatures. *Langmuir.* **2010**, *26*, 3981-3992.
12. Krishna, R.; van Baten, J. M., Highlighting a Variety of Unusual Characteristics of Adsorption and Diffusion in Microporous Materials Induced by Clustering of Guest Molecules. *Langmuir.* **2010**, *26*, 8450-8463.
13. Parker, D. H.; Bartram, M. E.; Koel, B. E. Study of High Coverages of Atomic Oxygen on the Pt(111) Surface. *Surf. Sci.* **1989**, *217*, 489-510.
14. Campbell, C. T.; Sellers, J. R. V. The Entropies of Adsorbed Molecules. *J. Am. Chem. Soc.* **2012,** *134*, 18109-18115.
15. Tait, S. L.; Dohnalek, Z.; Campbell, C. T.; Kay, B. D. N-Alkanes on Pt(111) and on C(0001)/Pt(111): Chain Length Dependence of Kinetic Desorption Parameters. *J. Chem. Phys.* **2006**, *125*, 234308-1-15.